Combining optical and electrical impedance techniques for quantitative measurement of confluence in MDCK-I cell cultures

Birgitte Freiesleben De Blasio[1,2], Morten Laane[2], Thomas Walmann[2], and Ivar Giaever[3]

BioTechniques 36:650-662 (April 2004)

A new method combining optical and electrical impedance measurements is described that enables submicroscopic cell movements to be monitored. The cells are grown on small gold electrodes that are transparent to light. This modified electrical cell-substrate impedance sensor (ECIS) allows simultaneous microscopic recording of both growth and motility, thus enabling cell confluence on the electrodes to be systematically correlated to the impedance in regular time intervals of seconds and for extended periods of time. Furthermore, the technique provides an independent measure of monolayer cell densities that we compare to calculated values from a theoretical model. We have followed the attachment and spreading behavior of epithelial Madin-Darby canine kidney strain I (MDCK-I) cell cultures on microelectrodes for up to 40 h. The studies reveal a high degree of correlation between the measured resistance at 4 kHz and the corresponding cell confluence in 4- to 6-h intervals with typical linear cross-correlation factors of r *equaling approximately 0.9. In summary, the impedance measured with the ECIS technique provides a good quantitative measure of cell confluence.*

INTRODUCTION

The electrical cell-substrate impedance sensing (ECIS) technique provides a simple and efficient interface for quantitative and dynamic monitoring of cell adhesion and spreading behaviors of cells on artificial surfaces. In this approach, cells are cultured directly on two gold electrodes, one microdisk electrode (diameter is approximately $25 \cdot 10^{-3}$ cm) and a substantially larger reference electrode deposited on the bottom of a tissue culture chamber (Figure 1). Weak AC currents are applied to the system, and the voltage across the electrodes is measured with a lock-in amplifier.

The design has two important features. (*i*) A 4-kHz frequency is used to eliminate any significant polarization of the electrodes. (*ii*) Because of the small electrode, the solution resistance is reduced and basically confined to a small volume near the microelectrode (1,2). Consequently, a highly sensitive sensor is created at the interface between the microelectrode and the solution. When cells attach to the small electrode, the low conductivity of the cell membranes forces the electrical field lines to bend around the cells, and the measured voltage increases.

ECIS is now a well-established technique. Not only can characteristic curves may be obtained for various cell strains, but the actions due to physical and chemical parameters may also be easily detected (3). In addition, the technique has been applied to measure transendothelial resistance (4), study cell behavior under flow (5), and in wound healing assays (6).

Studies of cell attachment and motility are usually performed with the use of laborious methods based on microscopy (7,8). These techniques require both storage of large amounts of data and time-consuming analysis. In contrast, the impedance measurement has the advantage of providing quantitative information about cell behavior in real time while being inherently sensitive to changes in the activities of single cells.

The impedance signals obtained with ECIS contain important information about cell spreading and motion. To extract the biological information, models have been published that translate the impedance variations into averaged morphological parameters in terms of transepithelial resistance, specific cell membrane capacitance, and cell-substrate separation (9,10). However, the degree of confidence in the model predictions must ultimately be tested experimentally by independent measurements of each of these morphological components.

Not much is known about the correlation between the cell's structural changes upon the electrode and the measured impedance. Here we describe a technique that combines ECIS impedance measurements with optical monitoring of cellular behavior on the electrode using subconfluent cultures of the epithelial Madin-Darby canine kidney strain I (MDCK-I) cells. Information about cell densities and the placement of cells on the electrode is correlated to the time-dependent resistance at 4 kHz. In addition, we have compared the measured cell densities with corresponding values obtained from a theoretical model of the current flow across the cell layer. The information acquired in this study is im-

[1]Copenhagen University, Copenhagen, Denmark, [2]University of Oslo, Oslo, Norway, and
[3]Rensselaer Polytechnic Institute, Troy NY, USA

portant for better interpretation of ECIS data, such as in connection with wound healing assays and for more widespread acceptance of the technique.

MATERIALS AND METHODS

Reagents

Dulbecco's modified Eagle's Medium (DMEM) and fetal calf serum (FCS) were obtained from Gibco (Paisely, UK), HEPES buffer was from Sigma (St. Louis, MO, USA), and L-glutamine was from Flow Laboratories (Irvine, UK). Tissue culture plastic dishes (75 cm^2) were bought from Nunc (Roskilde, Denmark).

The HEPES-buffered salt solution (HSS) contained 136 mM NaCl, 5 mM KCl, 1.2 mM $MgCl_2$, 1.2 mM $CaCl_2$, 11 mM bacto dextrose (Sigma), and 10 mM HEPES, pH 7.35. All chemicals were of analytical quality.

Cell Culture

MDCK cells strain I was provided by Prof. K. Prydz (The Biotechnological Centre, University of Oslo, Oslo, Norway). Cells were grown in 75 cm^2 standard tissue cultures bottles and kept in an NP-2 incubator (Nikon, Tokyo, Japan) at 37°C with 5% CO_2, in a humidified atmosphere. They were cultured in 10 mL DMEM with 2 mM L-glutamine and 5% FCS.

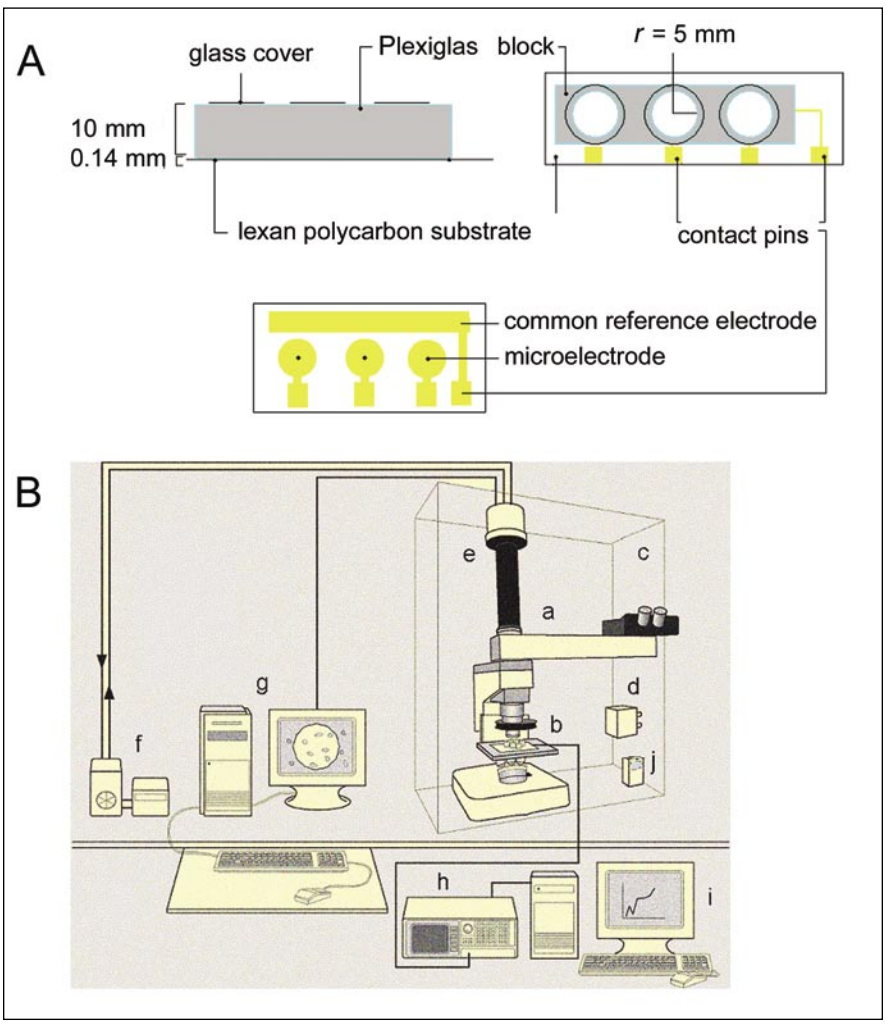

Figure 1. Electrode design and instrumentation. (A) Drawings of modified electrical cell-substrate impedance sensor (ECIS) well and electrode system. (B) The experimental setup. (a) Inverted optical microscope. (b) ECIS electrode system. (c) Plexiglas box. (d) Incubator. (e) Charge-coupled device (CCD) camera head. (f) CCD cooling pump. (g) Interfaced PC to control CCD camera. (h) Lock-in amplifier. (i) Interfaced computer to control ECIS measurement. (j) Dual-probe thermometer.

Twice a week, the confluent cultures were washed twice with phosphate-buffered saline (PBS) and split using trypsin/EDTA. The cells were seeded out in a concentration of 1:10–1:20.

ECIS Electrodes

Gold film electrodes were kindly supplied by Applied Biophysics (Troy, NY, USA). Thin golden film had been evaporated on a thin (approximately 0.14 mm) lexan polycarbonate substrate layer. Afterwards, the gold was delineated with an insulating film using a lithographic technique (11). The active microdisk electrodes had a final diameter of 250 µm. A cover was made to stabilize the highly flexible base. It was made from a 1-cm thick Plexiglas® block, which had drilled holes corresponding to the position of the individual electrodes on the lexan plate. The block was glued to the substrate using nontoxic silicon rubber (GE Silicones, Leverkusen, Germany) (Figure 1A). The completed electrode system comprised three individual wells (approximately 800 µL) with a surface area of 0.785 cm^2. During the experiments, the top of each well was completely sealed with a cover glass mounted with high vacuum grease (Dow Corning, Midland, MI, USA) to prevent the evaporation of liquid from the chamber.

Instrumentation

The experimental setup was build around an inverted optical microscope (Leitz Fluovert FS; E. Leitz, Wetzlar, Germany) (Figure 1B). The ECIS wells were placed in a specially designed holder and viewed under phase contrast with a Phaco2 10/0.45oel oil-immersion objective (Leitz Fluovert FU; E. Leitz). This objective combines the wide focus distance of 0.32 mm with a rather high optical resolution and no surface reflections. Thus, we were able to obtain detailed images of the cells by focusing through the plastic base of the wells. (The thin gold film is transparent to light.)

To control the temperature in the ECIS chamber, a Plexiglas box of approximately 1 m^3 was built around the microscope, and the box was heated using an NP-2 incubator. Part of the heated air

was blown directly over the glass cover to prevent dew formation. The microscope was mounted on a Model VH3048-OPT pneumatic vibration isolation table (Newport, Irvine, CA, USA). The temperature in the Plexiglas box and just outside the ECIS chamber was measured with a two-channel temperature probe (Memory Dual Thermo; Hanna Instruments, Singapore, Singapore).

The microscope was equipped with an ultra-sensitive charge-coupled device (CCD) camera head (Astro Cam TE4/W), and the CCD chip was cooled to 10°C using a cooling pump (Grant LTD 6/20; Grant Instruments Ltd., Barrington, Cambridge, UK). The camera was controlled from an interfaced PC using the CameraControl version 3.0 RC7 software program (LSR Astrocam, Cambridge, UK). The images were stored in 16-bit raw format for further processing.

The ECIS electrode system was connected to a lock-in amplifier and interfaced to a second PC. The communication was carried out via general purpose interface bus (GPIB) and controlled from a Microsoft® DOS-based program written in Turbo Pascal version 5.0 for this purpose by the authors. The resulting in-phase and out-of-phase voltages were converted into equivalent capacitances and resistances by treating the ECIS sample dish as a series resistor capacitor (RC) circuit.

Experimental Procedure

The ECIS dish was filled with approximately 1 mL solution consisting of 2/3 culture medium and 1/3 HSS solution. The latter was required to prevent the acidification of the liquid caused by the build up of CO_2 in the chamber. The cells were seeded out in about 1/20 of the concentration necessary to obtain confluence.

Due to the intense light, the temperature in the sealed ECIS container was higher than in the surrounding Plexiglas box. The temperature difference between the liquid in the chamber and outside the chamber was established from preliminary experiments to be about 5°C and stabilized within 15 min. Accordingly, the outer volume was heated to 32°C to provide a working temperature of 37°C to the cells.

Images were recorded each 60–70 s, and the electrodes were monitored from the time cells were seeded out up to 48 h. Due to the huge image files, the recordings had to be performed in intervals of 6–8 h, interrupted by short breaks to transfer data. The ECIS measurements were made at 4 kHz and in correspondence with the timing of the individual images.

Image Processing Procedure

Images were processed by converting the raw pictures into black-and-white outlines of the cells using the freeware program Scion Image release Beta 4.02 (Scion Corporation, Frederick, MD, USA). The border between the cell membrane and the medium was expressed as a dark halo line and revealed the approximate outline of each cell. The exact position of the cell membranes at time t' was found from the outline of the cells from the previous image (t' - 1), the image itself, and subtraction of the previous image from the next, (t' + 1) - (t' - 1). In some circumstances, particularly for cells with a spread-out morphology, it was necessary to subtract images with longer timespans.

RESULTS

The electrode design and instrumentation setup of the modified ECIS system are shown (Figure 1, A and B). Using this apparatus, we analyzed 5 recordings, including 3 early attachment assays and 2 recordings of a 15-h and a 32-h culture. From each measurement, 106–203 images were analyzed, with an average of 160 images. Initially, 10–20 cells of spherical shape were confined on the electrode, covering 4%–8% of the total electrode area, compared to 30%–50% at the end of the experiment. The numbers of cells changed in time due to cell proliferation and active movements between the electrode and the isolating surroundings.

Individual electrode systems have slightly different electrical characteristics, and the impedance measured using different electrodes is not directly comparable. Therefore, we often present data as normalized versus time, which enables much better comparisons between experiments. We focus on the resistive part of impedance because at 4 kHz cellular activity is mainly visible as changes in the resistance, while the

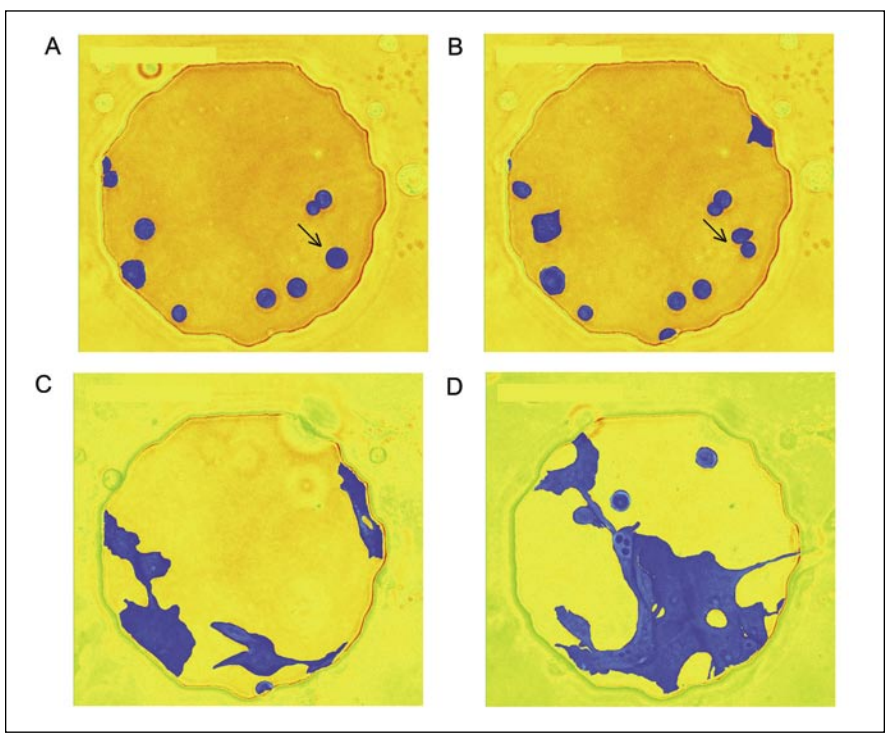

Figure 2. Micrographs of cells on the electrode. Four micrographs of the same culture recorded at (A) 20 min, (B) 90 min, (C) 11 h, and (D) 34 h after the culture was started. (A and B) The occurrence of a cell division within the first hour is indicated. Images are shown without further processing.

capacitive contribution to the impedance peaks at higher frequencies of around 40 kHz (9). The normalized resistance $R_{norm}(t)$ is defined by

$$R_{norm}(t) = \frac{R(t)}{R_0} \quad \text{[Eq. 1]}$$

where $R(t)$ is the measured resistance at time t, and R_0 is the the resistance measured when the cells were seeded out. The solution resistance is on the order of 1–1.1 kΩ, and the impedance of a naked electrode is 1.8–2.0 kΩ (4 kHz).

Attachment and Movement

The near-spherical cells acquired characteristic, flattened morphologies (12) typical for subconfluent epithelial cultures, with visible membrane ruffling within the first hour, followed by a general increase in cell areas, typically by a factor of 2–3 (Figure 2, A and B).

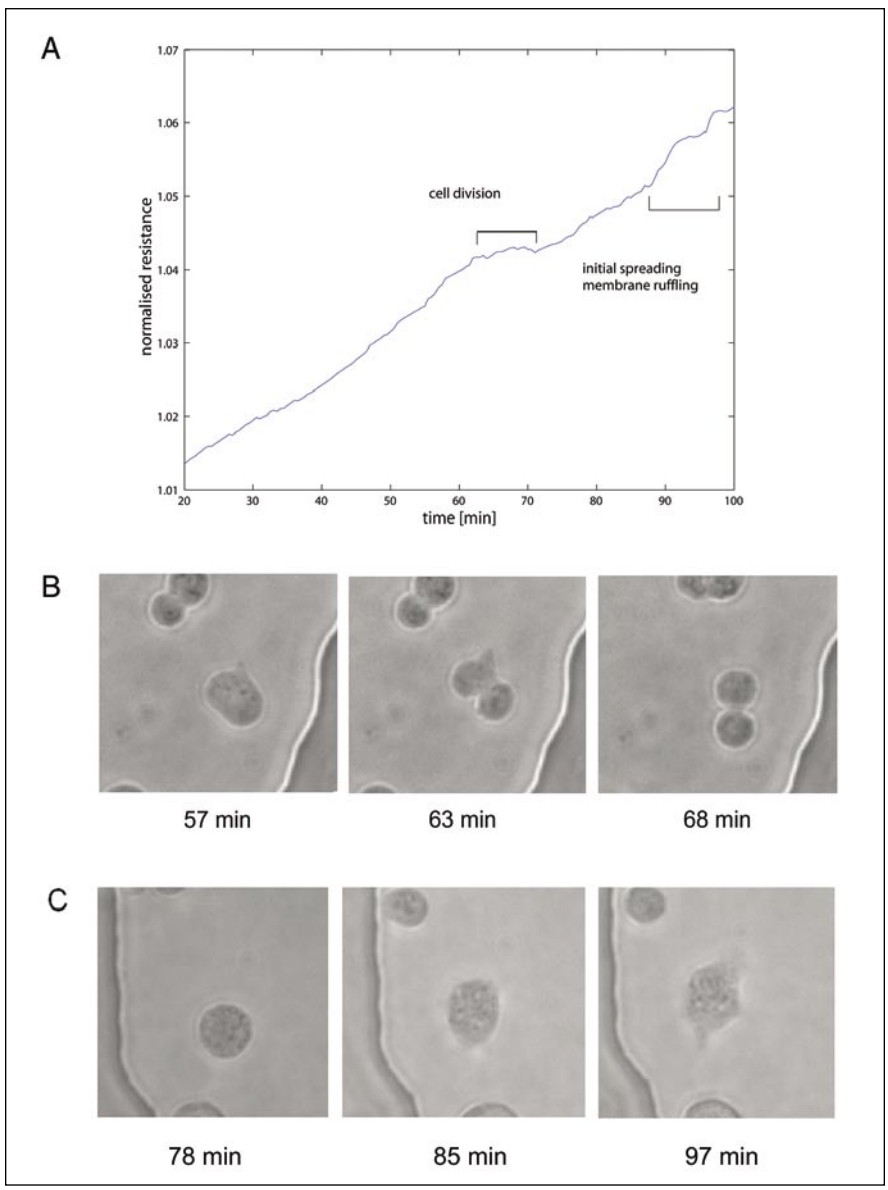

Figure 3. Impedance alterations and single-cell events during early recordings. (A) Normalized resistance of an early attachment assay plotted as a function of time starting when the cells were seeded. The occurrence of a cell division and the membrane ruffling/initial spread of a cell is indicated. (B) Three micrographs of the cell division referenced above. The time of the recording is shown to allow for comparison with the impedance graph in panel A. (C) Three micrographs with time points showing membrane ruffling and the beginning of a spreading cell.

Later stage attachment was characterized by the formation of small groups, or clusters, of cells (Figure 2, C and D). The clusters were connected by thin elongations to cells outside the electrode and pulled from different directions by the surrounding peripheral cells. The cluster movements appeared to be due to pulling by these cable connections from cells further apart. The cells in the center of the clusters seemed to play a passive role in these movements.

The impedance measurements allow single-cell events to be detected within the first 1–2 h (Figure 3). A plateau in the resistance curve is found to coincide with a chance cell division taking place on the electrode (Figure 2, A and B compared to Figure 3, A and B). This particular event was observed only once. In all three early recordings, membrane ruffling and the initial spreading of cells were found to correlate with a relative increase (gradient) in the resistance. During membrane ruffling, the clear halo ring surrounding the cell vanishes, and the cell becomes elongated (Figure 3, A and C). When the cells are completely spread, it is no longer possible to link changes in the resistance to individual cell behavior, such as resistance alterations caused by a cell leaving or entering the electrode. These movements, which occur at 20-min intervals, are effectively masked by the activity of the other cells. In late cultures, the cell movements sometimes result in breakage of the thin projections connecting two clusters, followed by a retraction of filopodium and a general contraction of the cells. Such major events are visible as a steep drop in the resistance covering the same period of time (Figure 4, A and B).

The cells moved with an average velocity of 1–3 µm/min. This is in agreement with previous reports of translocation speed of the cell line on plastic substrates (0.5–1 µm/min) (13). Rapid cellular movements were associated with elongated or rounded morphologies, while spread morphologies were connected with reduced cellular translocation. The morphology and motility of cells adhering to the gold electrodes were similar to the cellular behavior on the surrounding photoresistant substrate, in agreement with previous observations (14).

Correlating Impedance and Cell Density

Two representative examples of the correlation between measured resistance (top) and cell density on the electrode (bottom) are shown in Figure 5. Figure 5A is a record of an early culture and covers a timespan of 6.25 h. In the first 20 min, cells are dropping down on the electrode and making initial contact with the surface, which is seen as a steep increase in the cell density (Figure 5A, bottom). Apart from this initial phase, the resistance is found to be strongly correlated to the changes in cell confluence with a coefficient of $r = 0.92$. The correlation coefficient reported (Pearson's r) describes the linear association between the variables. We use this measure because the r value is comparable to the coefficient obtained from a general correlation procedure (15) that does not assume the two variables to be linearly associated.

Figure 5B shows a record of a late culture. In this case, the measurements started 32 h after the cells were seeded out and cover a timespan of 4 h. Again, we obtained a strong linear correlation of $r = 0.94$. Generally, the linear correlation coefficient obtained in a 4- to 6-h interval was of order $r \sim 0.9$, both in early and late cultures.

To visualize the association between the variables, we plot the degree of cell coverage as a function of the measured resistance in the examples above (Figure 6). The upper graph (Figure 6A) corresponds to the early culture (Figure 5A), when excluding the first 20 min of the recording. The bottom graph (Figure 6B) is made with the data from the late culture (Figure 5B). Linear fits of the data in a least-square sense give a slope of $\alpha = 0.23 \pm 0.02/k\Omega$ in Figure 5A and a somewhat larger slope of $\alpha = 0.32 \pm 0.02/k\Omega$ in Figure 5B. The 95% confidence intervals of the α estimates are given, assuming the variation to be normally distributed. The standard deviation of the points around the linear fit is $s_{reg} = 0.019$ in the early culture experiment, and $s_{reg} = 0.020$ in the late culture.

In the early phase when the cells attach to the electrode (Figure 6A, left), the linear association between the cell confluence and the resistance is particularly pronounced. At later phases, the data points do not fall directly on a straight line. It is important to note that the impedance is affected by the vertical separation between the cells and the substrate. Thus, cell movements in the z-plane perpendicular to the electrode will be expected to create fluctuations around the average linear behavior.

Model Calculation of Cell Density

Wegener et al. (16) used a theoretical model of the current flow across the

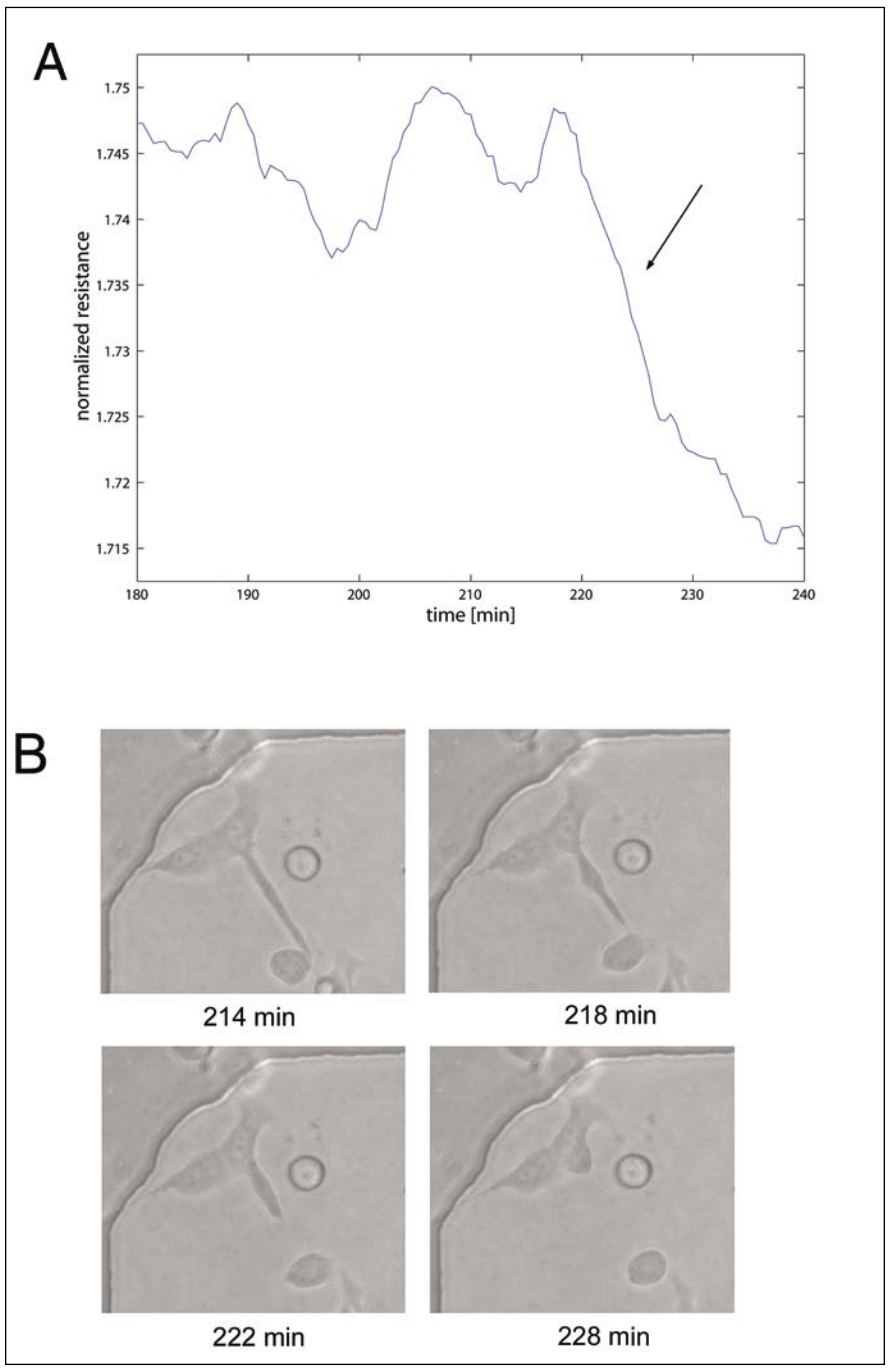

Figure 4. Impedance changes during cluster separation in late cultures. (A) The resistance plotted as a function of time of a late culture. The recording was initiated 32 h after the cells were seeded out, and time is referenced according to this point. The cluster separation is indicated with an arrow. (B) Four micrographs showing the cluster separation. The recording time is listed to allow for comparison with panel A.

interface (17) to predict cell coverage on the electrode from the normalized impedance. In the references above, both the model and the method to extract cell densities have been extensively discussed. We have used the morphological characteristics of MDCK-I cells and the normalized impedance Z_e obtained from the empty electrode to calculate the expected normalized Z_e for a given degree of cell coverage:

$$\frac{1}{Z_c} = \frac{1}{Z_e}\left\{\frac{Z_e}{Z_m + Z_e} + \frac{\frac{Z_m}{Z_e + Z_m}}{\frac{\gamma r_c}{2}\frac{I_0(\gamma r_c)}{I_1(\gamma r_c)} + R_b\left(\frac{1}{Z_e} + \frac{1}{Z_m}\right)}\right\}$$

$$\approx \frac{1}{Z_e}\left\{\frac{Z_e}{Z_m + Z_e} + \frac{\frac{Z_m}{Z_e + Z_m}}{\frac{\gamma r_c}{2}\frac{I_0(\gamma r_c)}{I_1(\gamma r_c)}}\right\} \quad \text{[Eq. 2]}$$

and

$$\gamma = \sqrt{\rho/h}\ \sqrt{(1/Z_e) + (1/Z_m)}\ .$$

Here Z_m is the specific membrane impedance, R_b the barrier function, r_c the average cell radius, ρ the resistivity of the solution, and h the average cell-substrate separation. In the present context, we will neglect the resistance from the current flow between the cells (i.e.. $R_b = 0$) because we are only concerned with subconfluent cultures.

In Figure 7, the normalized resistance has been calculated in this way as a function of cell coverage (thick blue line). We have inserted morphological data of MDCK-I cell cultures obtained from another study (18) in the model. In this figure, the normalized resistance is plotted as a function of the cell density of four different registrations (colored circles); each circle represents mean values in intervals of 15 min. Note that the relationship is not purely linear and, in accordance with the data, predicts a steeper slope for higher cell confluence. However, a characteristic difference between the densities predicted by the model and the experimentally obtained values is seen, even with relative errors as high as 40% for low-density recordings.

DISCUSSION

The ECIS technique is a highly versatile tool with a unique potential to study cell adhesion, cell motility, the action of chemical or physical factors, and virus infections, etc., upon cells, cell cycles, and numerous other dynamic processes on the microscopic level. To interpret the measured impedance, the information content of the time series must be explained in terms of biologically relevant measures such as structural cell changes that occur during the experiment. Specifically, in connection with sparse cultures, such as wound healing assays, it is essential to quantify the relationship between the impedance and the cell area. We therefore developed a method that combines the ECIS with an optical microscope.

We found a strong positive correlation between the measured resistance at 4 kHz and the degree of cell coverage on the electrode. We obtained linear cross-correlation coefficients of $r \sim 0.9$ in 4- to 6-h registrations, excluding the primary half hour in which the cells make initial contact with the surface. These results imply that approximately 80% $r^2 \sim 0.8$ of the observed variation in the resistance can be accounted for by changes in electrode cell densities. It appears that the correlation is equally strong in early and late cultures and therefore independent of whether the cells have rounded or spread morphology. This result is in good agreement with a recent study, in which a linear relationship between the numbers of fibroblast cells on the electrode and the resistance (4 kHz) was obtained (19).

In early cultures, we found coincidence between membrane ruffling and short-lived (5–10 min) gradients in the resistance. In one experiment, a chance cell division took place within the first hour after the cells were seeded, which coincided with a temporary plateau in the resistance. Once the cells had acquired

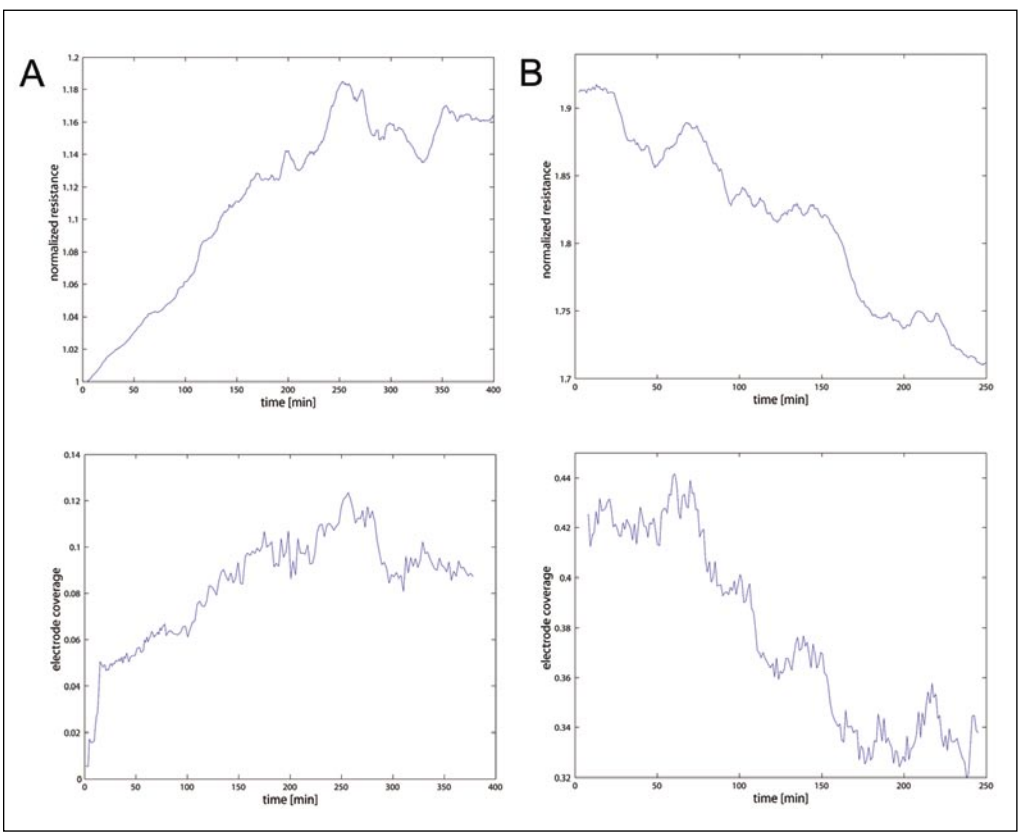

Figure 5. Correlation between resistance and cell coverage. The normalized resistance plotted as a function of time (upper panel), and the electrode coverage plotted as a function of time (lower panel). (A) An early culture, the linear cross-correlation factor was found to be $r = 0.92$, when excluding the first 20 min in the analysis. (B) A late culture started 32 h after the cells were seeded out. The cross-correlation factor was found to be $r = 0.94$.

spread morphology, the impedance change could no longer be attributed to single-cell events. However, by studying the cluster dynamics of later cultures, we observed a steep drop in the resistance that corresponded to breakage of elongated contacts between two aggregates of cells. This observation may explain the large impedance changes that are occasionally seen, especially in sparse cultures.

In an attempt to verify the procedure, we compared experimental data from four different registrations to theoretical calculations of cell densities based on the measured resistance. This model accounts for the general trend and agrees well with the empirical data, considering that many relevant factors are not included. There are at least four possibilities to consider for this discrepancy. (*i*) The impedance is affected not only by the horizontal coverage but also by the vertical displacement of the cells. The resistance will increase when the vertical separation between the basolateral membrane and the substrate get smaller. (*ii*) The model gives only a rough description of the current flow across the interface. In addition, the current flow from a semi-covered electrode is probably influenced by the open space on the electrode in a way that is not accounted for in the model. (*iii*) Some inaccuracy in estimating the cell densities is expected, which relates to the processing of images. Finally, (*iv*) in these experiments, it appears that a cell situated in the electrode periphery contributes more to the resistance than a cell of the same size located in the center of the electrode. This tendency could be a result of higher current densities at the electrode edges, which are generated as a consequence of the geometry of the microelectrode (2). However, this effect is expected to be of minor importance because the impedance at the interface is of order ~10 kΩ (reactance ~8 kΩ and resistance ~2 kΩ) and a factor 10 larger than the solution resistance of ~1 kΩ.

A better understanding of the actual current density would represent an important step toward a more precise interpretation of these experiments. One might use nonliving materials (e.g., by depositing microflakes) with known areas on different positions of the electrode and then measure the resulting impedance. This procedure would prevent variations in vertical separation from disturbing the measurements.

Further studies might also involve experiments at 40 kHz to correlate the capacitance with the cell density in a similar way. At this frequency, the rapidly

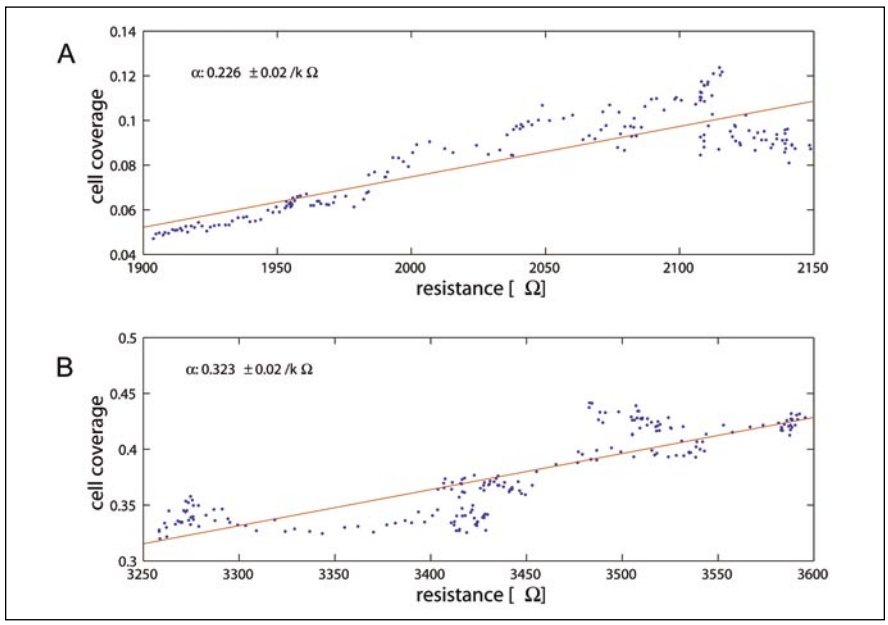

Figure 6. Cell coverage as a function of resistance. (A) Plot of cell coverage versus resistance of the early culture, corresponding to Figure 5A. The red line shows the best linear fit of the data. (B) Plot of cell coverage versus resistance of the late culture, corresponding to Figure 5B. Again the red line indicates the best linear fit of the data.

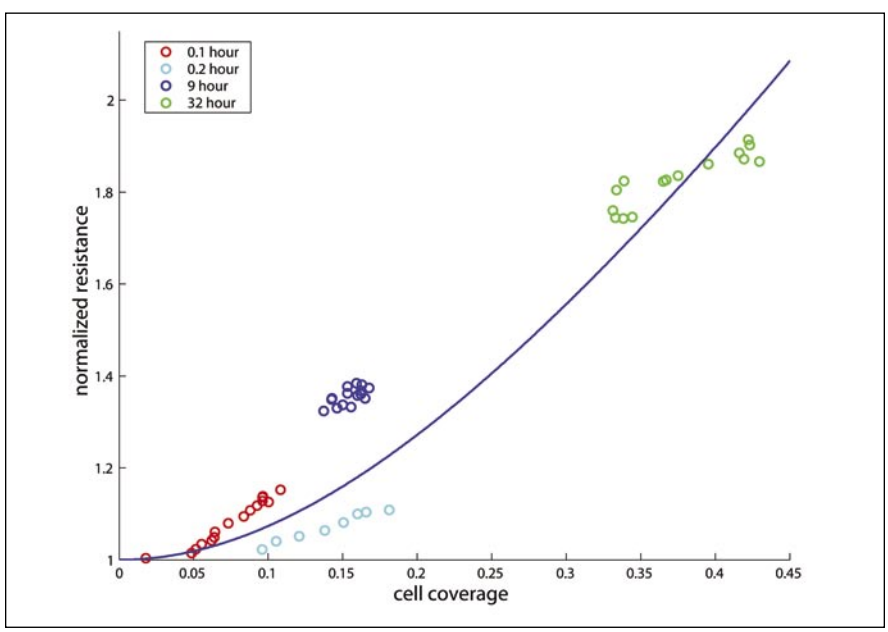

Figure 7. Theoretical prediction of cell coverage. Theoretical curve of the normalized resistance plotted as a function of cell coverage on the electrode. The parameter values used to generate the graph were estimated in a previous study (17): average cell-substrate separation h = 5 nm, specific cell membrane capacitance C_m = 5 μF/cm^2. The resistivity of the solution was set to ρ = 54 Ω cm^2 in accordance with previous measurements (1). Normalized resistance and corresponding cell density are shown for four different registrations with circles (red, cyan, blue, and green). Time points indicate when the recordings were initiated with respect to the start of the culture. Each circle corresponds to average values obtained in 15 min time intervals.

changing field prevents the current from flowing under the cells, which effectively reduces the importance of the cell-electrode separation. Modeling by Wegener et al. (16) suggests that the capacitance at this frequency shows a linear relationship with the degree of cell coverage on the electrode. Because of extensive handling of the electrodes, the measured capacitance was a factor of about 10 smaller than normal; we therefore decided to focus on the low frequency.

Epithelial MDCK cells, which were used in the present study, are known to interact strongly with the substrate and neighboring cells (1,2). The method is easily generalized to other types of epithelia and endothelia, and we expect to find a strong correlation between resistance and cell coverage in other such cultures. It has been found that cell-cell adhesion can reduce cell-substrate adhesion substantially in epithelial cells (20). However, the present experimental setup is insufficient to address this issue, and the effect is supposedly of minor importance in sparse cultures.

Finally, the combined technique cannot be used to study confluent cell layers because the impedance changes are then mainly caused by subtle changes in the cell-substrate separation. These variations are far below the resolution power of a conventional optical microscope. It appears possible, although technically complicated, to combine reflection contrast microscopy (21) with ECIS. This and a number of similar techniques are able to measure vertical displacement changes of 5–10 nm and could serve as a means to validate the theoretical model.

ACKNOWLEDGMENTS

Dr. B.F. De Blasio would especially like to thank Professor Jens-Gustav Iversen at the Physiological Department and Professor Jens Feder and Professor Torstein Jøssang at the Physics Department (Oslo University) for their hospitality during her stays in Oslo.

REFERENCES

1. **Pons, S. and M. Fleischmann.** 1987. The behavior of microelectrodes. Anal. Chem. *59*:1391A-1399A.
2. **Grimnes, S. and Ø.G. Martinsen.** 2000. Geometrical analysis, p. 127-152. *In* Bioimpedance and Bioelectricity Basics. Academic Press, Cornwall, UK.
3. **Noiri, E., A. Nakao, K. Uchida, H. Tsukahara, M. Ohno, T. Fujita, S. Brodsky, and M.S. Goligorsky.** 2001. Oxidative and nitrosative stress in acute renal ischemia. Am. J. Physiol. Renal Physiol. *281*:F948-F957.
4. **Tiruppathi, C., A.B. Malik, P.J. Del Vecchio, C.R. Keese, and I. Giaever.** 1992. Electrical method for detection of endothelial cell shape change in real time: assessment of endothelial barrier function. Proc. Natl. Acad. Sci. USA *89*:7919-7923.
5. **Phelps, J.E. and N. DePaola.** 2000. Spatial variations in endothelial barrier function in disturbed flows in vitro. Am. J. Physiol. Heart Circ. Physiol. *278*:H469-H476.
6. **Wegener, J., C.R. Keese, and I. Giaever.** 2002. Recovery of adherent cells after in situ electroporation monitored electrically. BioTechniques *33*:348-352.
7. **Waterman-Storer, C.M., W.C. Salmon, and E.D. Salmon.** 2000. Feedback interactions between cell-cell adherens junctions and cytoskeletal dynamics in newt lung epithelial cells. Mol. Biol. Cell *11*:2471-2483.
8. **Zamir, E., M. Katz, Y. Posen, N. Erez, K.M. Yamada, B.Z. Katz, S. Lin, D.C. Lin, et al.** 2000. Dynamics and segregation of cell-matrix adhesions in cultured fibroblasts. Nat. Cell Biol. *2*:191-196.
9. **Giaever, I. and C.R. Keese.** 1991. Micromotion of mammalian cells measured electrically. Proc. Natl. Acad. Sci. USA *88*:7896-7900.
10. **Lo, C.M., C.R. Keese, and I. Giaever.** 1995. Impedance analysis of MDCK cells measured by electric cell-substrate impedance sensing. Biophys. J. *69*:2800-2807.
11. **Giaevier, I. and C.R. Keese.** 1986. Use of electrical fields to monitor the dynamical aspects of cell behavior in tissue culture. IEEE Trans. Biomed. Eng. *33*:242-247.
12. **Koller, M.R. and E.T. Papoutsakis.** 1995. Cell adhesion in animal cell culture: physiological and fluid-mechanical implications. Bioprocess. Technol. *20*:61-110.
13. **Kolega, J., M.S. Shure, W.T. Chen, and N.D. Young.** 1982. Rapid cellular translocation is related to close contacts formed between various cultured cells and their substrata. J. Cell Sci. *54*:23-34.
14. **Hadjout, N., G. Laevsky, D.A. Knecht, and M.A. Lynes.** 2001. Automated real-time measurement of chemotactic cell motility. BioTechniques *31*:1130-1138.
15. **Altman, D.B.** 1990. Relation between two continuous variables, p. 277-321. *In* Practical Statistics for Medical Research. CRC Press, New York.
16. **Wegener, J., C.R. Keese, and I. Giaever.** 2000. Electric cell-substrate impedance sensing (ECIS) as a noninvasive means to monitor the kinetics of cell spreading to artificial surfaces. Exp. Cell Res. *259*:158-166.
17. **Giaever, I. and C.R. Keese.** 1991. Micromotion of mammalian cells measured electrically. Proc. Natl. Acad. Sci. USA *88*:7896-7900.
18. **De Blasio, B.F., J.-A. Rottingen, K. Larsen Sand, I. Giaever, and J.G. Iversen.** Global, synchronous oscillations in cytosolic calcium and adherence in bradykinin-stimulated Madin-Darby canine kidney cells. Acta Physiol. Scand. (In press).
19. **Xiao, C., B. Lahance, G. Sunahara, and J.H.T. Luong.** 2002. An in-depth analysis of electrical cell-substrate impedance sensing to study the attachment and spreading of mammalian cells. Anal. Chem. *74*:1339.
20. **Grosheva, I., M. Shtitman, M. Elbaum, and A.D. Bershadsky.** 2000. p120 catein affects cell motility via modulation of activity of Rho-family GTPases: a link between cell contact formation and regulation of cell locomotion. J. Cell Sci. *114*:695-707.
21. **Verschueren, H.** 1985. Interference reflection microscopy in cell biology: methodology and applications. J. Cell Sci. *75*:279-301.

Received 14 November 2003; accepted 22 January 2004.

Address correspondence to:

Birgitte Freiesleben De Blasio
Institute for Nutrition Research
Sognvannsveien 9
P.O.Box 1046, Blindern
NO-0316 Oslo, Norway
e-mail: birgitte.deblasio@basalmed.uio.no